Int. J. Solids Structures Vol. 29, No. 24, pp. 3251–3267, 1992
Printed in Great Britain.

0020–7683/92 $5.00 + .00

THE BEHAVIOR OF CRACKED CROSS-PLY COMPOSITE LAMINATES UNDER SHEAR LOADING

C.-L. TSAI and I. M. DANIEL
Robert R. McCormick School of Engineering and Applied Science,
Northwestern University, Evanston, IL 60208, U.S.A.

(*Received* 21 *May* 1991; *in revised form* 5 *March* 1992)

Abstract—An interlaminar-shear-stress analysis developed earlier by Tsai *et al.* (1990, *Micro-cracking-Induced Damage in Composites*) for a $[\phi_m/\theta_n]_s$ bi-directional composite laminate is used to solve the case of a cross-ply $[0_m/90_n]_s$ laminate with the 90° layer only or both layers cracked under pure shear loading. Strains, forces and laminate shear modulus reduction due to matrix cracking were obtained. Experimental results for shear modulus as a function of crack densities were obtained by a simple shear test and they agree very well with the theoretical prediction.

INTRODUCTION

A great deal of work has been reported to date on axial stiffness degradation in composite laminates due to matrix cracking. Highsmith and Reifsnider (1982) and Ogin *et al.* (1985) used a shear lag analysis. Talreja (1985) used stiffness–damage relationships based on continuum mechanics and internal variables; Hashin (1985, 1987) used variational principles; Lim and Hong (1989) proposed a modified shear lag analysis; Lee (1988) and Lee and Daniel (1990) proposed another modified shear lag analysis; an interlaminar-shear-stress analysis was developed by Tsai *et al.* (1990); Dvorak *et al.* (1985) and Laws and Dvorak (1988) used statistical fracture mechanics; Caslini *et al.* (1987), Sun and Jen (1987), Allen *et al.* (1988) and Groves *et al.* (1987) used finite element methods; Aboudi *et al.* (1988) used a second-order Legendre expansion for displacements and the finite element method; Tan and Nuismer (1989) used the state of stress in a cracked laminate and a fracture criterion based on energy considerations. Relatively few investigations have dealt with shear modulus reduction. Hashin (1985), Tan and Nuismer (1989) and Herakovich *et al.* (1988) analysed cross-ply laminates with cracks in the 90° layer under in-plane normal and shear loading but they did not offer experimental data for comparison. Yaniv *et al.* (1989) conducted simple shear tests to monitor the shear modulus reduction during fatigue loading. An improved simple shear test was described recently by Tsai and Daniel (1991).

A general interlaminar-shear-stress analysis was developed earlier for a $[\phi_m/\theta_n]_s$ bi-directional composite laminate by Tsai *et al.* (1990) which does not start with the usual assumption of the classical shear lag analysis that the interlaminar shear stresses are proportional to the displacement difference between the two layers. However, the analysis shows agreement with this assumption. From this analysis a system of governing equations was derived that involves only in-plane displacements in both layers, based on equilibrium, continuity and boundary conditions. This system can be solved to analyse cross-ply laminates $[0_m/90_n]_s$, with one or both layers cracked under different loading conditions by imposing appropriate boundary conditions. The cracks in the matrix are assumed to be normal to the x–y plane (Fig. 1), although it was found experimentally by Highsmith and Reifsnider (1982), Groves *et al.* (1987) and Allen *et al.* (1988) that this is not always true. Predictions of stiffness reduction due to cracks in both layers were obtained and proved experimentally by Daniel and Tsai (1991). In this work the reductions of shear modulus due to cracks in the 90° layer only and due to cracks in both layers are predicted and verified experimentally. Although the approach used here is fundamentally different, the prediction for shear modulus reduction due to cracks in the 90° layer is identical with that of Hashin (1985) and Tan and Nuismer (1989) and agrees very well with experimental data.

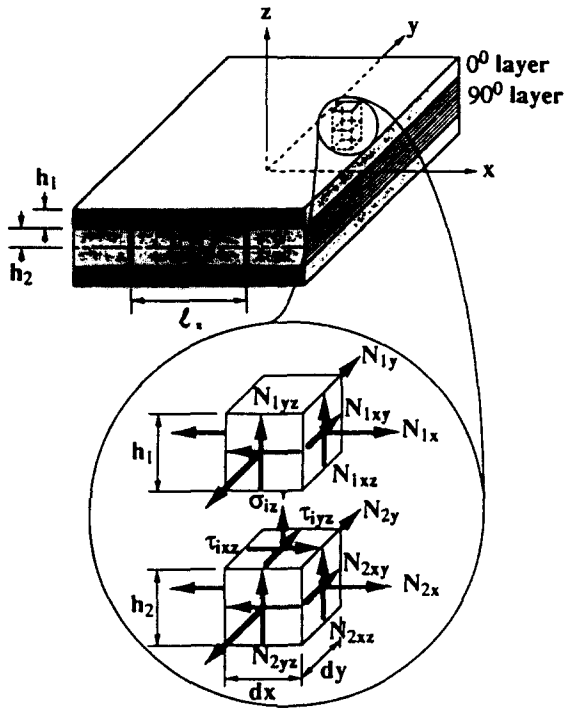

Fig. 1. Cross-ply $[0_m/90_n]_s$ laminate with cracked 90° layer and free body diagrams of elements.

GOVERNING EQUATIONS FOR CROSS-PLY LAMINATES

For cross-ply laminates the interlaminar-shear-stress analysis provides the relationships among the through-the-thickness average displacements of each layer in the form of the following partial differential equations obtained by Tsai *et al.* (1990):

$$Q_{22}\bar{u}_{2,xx}+Q_{12}\bar{v}_{2,xy}+Q_{66}(\bar{u}_{2,yy}+\bar{v}_{2,xy})=\frac{H_{11}}{h_2}(\bar{u}_2-\bar{u}_1), \tag{1}$$

$$Q_{11}\bar{u}_{1,xx}+Q_{12}\bar{v}_{1,xy}+Q_{66}(\bar{u}_{1,yy}+\bar{v}_{1,xy})=\frac{H_{11}}{h_1}(\bar{u}_1-\bar{u}_2), \tag{2}$$

$$Q_{11}\bar{v}_{2,yy}+Q_{12}\bar{u}_{2,xy}+Q_{66}(\bar{v}_{2,xx}+\bar{u}_{2,xy})=\frac{H_{22}}{h_2}(\bar{v}_2-\bar{v}_1), \tag{3}$$

$$Q_{22}\bar{v}_{1,yy}+Q_{12}\bar{u}_{1,xy}+Q_{66}(\bar{v}_{1,xx}+\bar{u}_{1,xy})=\frac{H_{22}}{h_1}(\bar{v}_1-\bar{v}_2), \tag{4}$$

where Q_{11}, Q_{12}, Q_{22} and Q_{66} are stiffness parameters of the basic lamina, with $Q_{66}=G_{12}$ (in-plane shear modulus) in our case; $\bar{u}_1$, $\bar{v}_1$, $\bar{u}_2$ and $\bar{v}_2$ are average displacements of the 0° and 90° layers in the x- and y-directions, h_1 is thickness of the 0° layer and h_2 is the half thickness of the 90° layer (Fig. 1). H_{11} and H_{22} are interlaminar-shear-stress parameters given by

$$H_{11}=\frac{3G_{13}G_{23}}{h_2G_{13}+h_1G_{23}}, \quad H_{22}=\frac{3G_{13}G_{23}}{h_1G_{13}+h_2G_{23}},$$

where G_{13} and G_{23} are out-of-plane shear moduli of the basic lamina.

The left-hand sides of eqns (1)–(4) are gradients of stress which can be related to interface shear stresses. The right-hand sides are differences of displacement between the two layers. The interlaminar-shear-stress parameters can be viewed physically as effective

shear stiffnesses relating interface shear stresses and average displacement differences between the two layers.

LAMINATES WITH CRACKS IN 90 LAYER

Stress analysis

The stresses and strains in the undamaged laminate are independent of the location coordinates x and y. This means that the displacements $\bar{u}_1$, $\bar{v}_1$, $\bar{u}_2$ and $\bar{v}_2$ should be linear and, under pure shear loading, should give no rise to normal strains or stresses along the x- and y-axes:

$$\bar{u}_1 = C_1 y, \tag{5}$$

$$\bar{v}_1 = C_2 x, \tag{6}$$

$$\bar{u}_2 = C_3 y, \tag{7}$$

$$\bar{v}_2 = C_4 x. \tag{8}$$

When only the 90° layer is cracked with a crack spacing ℓ_x, the disturbance in the solution above will only be a function of x (Fig. 2). Furthermore, only the displacement components $\bar{v}_1$ and $\bar{v}_2$ will be disturbed in order to maintain the pure shear state of strain. This disturbance is a hyperbolic term as suggested by Tsai *et al.* (1990) for the governing equations (1)–(4). Thus, for the cracked laminate we have:

$$\bar{u}_1 = C_1 y, \tag{9}$$

$$\bar{v}_1 = C_2 x + C_5 \sinh(\alpha x), \tag{10}$$

$$\bar{u}_2 = C_3 y, \tag{11}$$

$$\bar{v}_2 = C_4 x + C_6 \sinh(\alpha x), \tag{12}$$

where α is the eigenvalue and C_i ($i = 1, 2, \ldots, 6$) are unknown coefficients to be determined. Substituting eqns (9)–(12) into eqns (1)–(4), we obtain:

$$C_1 = C_3, \tag{13}$$

$$C_2 = C_4, \tag{14}$$

$$\alpha^2 = \frac{H_{22}}{Q_{66}}\left(\frac{1}{h_1} + \frac{1}{h_2}\right), \tag{15}$$

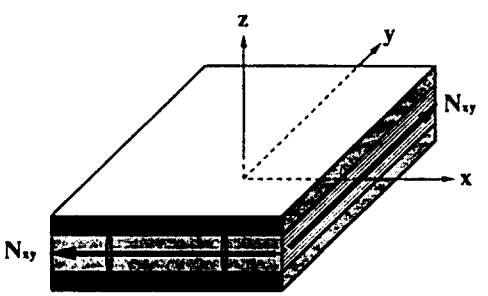

Fig. 2. Cracked cross-ply $[0_m/90_n]_s$ laminate under pure shear loading.

$$C_5 = -\frac{h_2}{h_1} C_6. \tag{16}$$

The displacements then become:

$$\bar{u}_1 = C_1 y, \tag{17}$$

$$\bar{v}_1 = C_2 x - \frac{h_2}{h_1} C_6 \sinh(\alpha x), \tag{18}$$

$$\bar{u}_2 = C_1 y, \tag{19}$$

$$\bar{v}_2 = C_2 x + C_6 \sinh(\alpha x), \tag{20}$$

which result in zero normal strains. Shear strains are derived as:

$$\gamma_{1xy} = C_1 + C_2 - \frac{h_2}{h_1} C_6 \alpha \cosh(\alpha x), \tag{21}$$

$$\gamma_{2xy} = C_1 + C_2 + C_6 \alpha \cosh(\alpha x). \tag{22}$$

From these shear strains, we obtain shear forces in each layer as follows:

$$N_{1xy} = h_1 Q_{66} \left[C_1 + C_2 - \frac{h_2}{h_1} C_6 \alpha \cosh(\alpha x) \right] \tag{23}$$

$$N_{2xy} = h_2 Q_{66} [C_1 + C_2 + C_6 \alpha \cosh(\alpha x)]. \tag{24}$$

All normal forces are zero.

If N_{xy} is the shear force per unit width (or length) applied to the laminate, then at the crack boundary $x = \pm \ell_x/2$ we have $N_{1xy} = N_{xy}/2$ and $N_{2xy} = 0$. This condition yields:

$$C_6 = -\frac{N_{xy}}{Q_{66} 2(h_1 + h_2) \alpha \cosh(\alpha \ell_x/2)}, \tag{25}$$

$$C_1 + C_2 = \frac{N_{xy}}{Q_{66} 2(h_1 + h_2)}. \tag{26}$$

There is an infinite number of pairs of solutions for C_1 and C_2, because of the rigid body rotation. However, the sum $(C_1 + C_2)$ is always a constant.

The shear strains and shear forces in each layer become:

$$\gamma_{1xy} = \frac{N_{xy}}{Q_{66} 2(h_1 + h_2)} \left[1 + \frac{h_2}{h_1} \frac{\cosh(\alpha x)}{\cosh(\alpha \ell_x/2)} \right], \tag{27}$$

$$\gamma_{2xy} = \frac{N_{xy}}{Q_{66} 2(h_1 + h_2)} \left[1 - \frac{\cosh(\alpha x)}{\cosh(\alpha \ell_x/2)} \right], \tag{28}$$

$$N_{1xy} = \frac{N_{xy} h_1}{2(h_1 + h_2)} \left[1 + \frac{h_2}{h_1} \frac{\cosh(\alpha x)}{\cosh(\alpha \ell_x/2)} \right], \tag{29}$$

$$N_{2xy} = \frac{N_{xy}h_2}{2(h_1+h_2)}\left[1 - \frac{\cosh(\alpha x)}{\cosh(\alpha \ell_x/2)}\right]. \tag{30}$$

Shear modulus reduction

The shear strain in the laminate defined as the average shear strain in the undamaged layer is:

$$\bar{\gamma}_{xy} = \left(\int_{-\ell_x/2}^{\ell_x/2} \gamma_{1xy}\,dx\right)\Big/\ell_x = \frac{N_{xy}}{\rho_G Q_{66} 2(h_1+h_2)}, \tag{31}$$

where ρ_G is the shear modulus reduction ratio:

$$\rho_G = \left[1 + \frac{2}{\ell_x}\frac{h_2}{h_1}\frac{1}{\alpha}\tanh\left(\alpha\frac{\ell_x}{2}\right)\right]^{-1}. \tag{32}$$

Experimental results

The material used was a graphite/epoxy (AS4/3501-6, Hercules, Inc.) with the following properties:

longitudinal modulus: E_1 = 145 GPa (21.0 Msi),
transverse modulus: E_2 = 10.6 GPa (1.54 Msi),
in-plane shear modulus: G_{12} = 6.9 GPa (1.00 Msi),
out-of-plane transverse shear modulus: G_{13} = 7.0 GPa (1.01 Msi),
out-of-plane transverse shear modulus: G_{23} = 3.7 GPa (0.54 Msi),
major Poisson's ratio: ν_{12} = 0.27.

Composite cross-ply coupons of $[0/90_2]_s$ and $[0/90_4]_s$ layup were tested in a fixture specially developed by Yaniv *et al.* (1989) (Fig. 3). The specimens were standard straight-edge coupons, 2.54 cm (1 in.) wide and 23 cm (9 in.) long. When the specimen is mounted in the fixture, two 1.27 cm (0.5 in.) wide and 2.54 cm (1 in.) long strips of the coupon are exposed as the test section and are subjected to shear loading. The relative motion of the central rails with respect to the outer rails is measured with an extensometer as shown in Fig. 3.

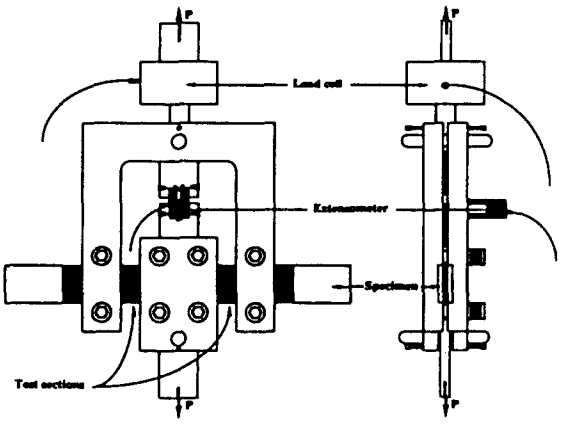

Fig. 3. Simple shear test fixture.

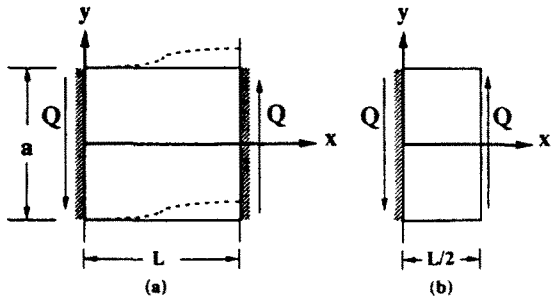

Fig. 4. Test section under simple shear analysed as (a) fixed-ended beam and (b) cantilever beam.

Each test section can be viewed as a fixed-end beam under shear loading, which can then be analysed as two cantilever beams of half the length of the original beam (Fig. 4). By using the Timoshenko beam theory the displacement in the y-direction is obtained by Tsai and Daniel (1991) as a function of both the axial modulus, $\bar{E}_x$, and the in-plane shear modulus $\bar{G}_{xy}$ of the laminate:

$$v = \frac{Q}{k^2 \bar{G}_{xy} h a} x + \frac{12Q}{\bar{E}_x h a^3}\left(\frac{L}{2} - \frac{x}{3}\right)\frac{x^2}{2}, \tag{33}$$

where h = specimen thickness, a = width, L = test section length.

The shear correction factor k^2 for cross-ply laminates was shown by Tsai *et al.* (1990) to be equal to 5/6, as in the case of isotropic materials.

From eqn (33) we obtain the deflection of the cantilever beam of Fig. 4(b) as

$$v_{x=L/2} = \frac{3Q}{5\bar{G}_{xy} h a} L + \frac{QL^3}{2\bar{E}_x h a^3}, \tag{34}$$

which leads to

$$\bar{G}_{xy} = \frac{6QL\bar{E}_x a^2}{10 v_{x=L/2}\bar{E}_x h a^3 - 5QL^3}. \tag{35}$$

In the test we measure the relative deflection δ of the center rails with respect to the outer rails and the applied load P. In eqn (35)

$$v_{x=L/2} = \delta/2, \tag{36}$$

$$Q = P/2, \tag{37}$$

thus,

$$\bar{G}_{xy} = \frac{6PL\bar{E}_x a^2}{10\delta\bar{E}_x h a^3 - 5PL^3}. \tag{38}$$

The laminate axial modulus $\bar{E}_x$ has been obtained by Tsai *et al.* (1990) as a function of transverse crack spacing. If we neglect the Poisson ratio effect, we have:

$$\bar{E}_x = \bar{E}_x^0\left[1 + \frac{h_2 E_2}{h_1 E_1}\frac{2}{\alpha_1 \ell_x}\tanh\left(\frac{\alpha_1 \ell_x}{2}\right)\right]^{-1}, \tag{39}$$

where

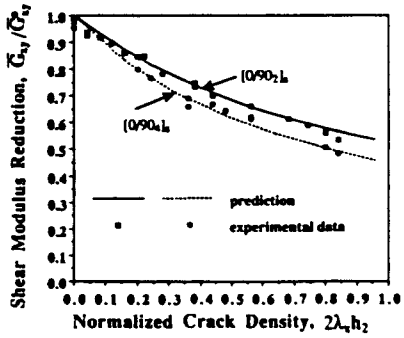

Fig. 5. Shear modulus reduction as a function of normalized crack density in 90° layer of cross-ply graphite/epoxy laminates.

$$\alpha_1 = \sqrt{H_{11}\left(\frac{1}{E_1 h_1} + \frac{1}{E_2 h_2}\right)} \quad \text{and} \quad \bar{E}_x^0 = \frac{2h_1 E_1 + 2h_2 E_2}{h}.$$

Results for the shear modulus reduction for the two laminates tested are plotted versus transverse crack density $\lambda_x = 1/\ell_x$ and compared with theoretical predictions in Fig. 5. The agreement is excellent.

LAMINATES WITH CRACKS IN BOTH LAYERS

Stress analysis

In the preceding case a closed form solution was obtained for a cross-ply laminate with one cracked layer by simply adding a hyperbolic term to the undisturbed solution for the undamaged laminate. In the case of laminates with both the 0 and 90° layers cracked this type of superposition is not justified and we cannot obtain an analytical solution that satisfies all boundary conditions. For this reason, a finite difference iteration method was used to solve the general system of governing equations to satisfy the boundary conditions of a cross-ply laminate under pure shear loading with all plies cracked. The initial guess needed in the finite difference iteration procedure was provided by superposition of the solution of the previous case in two directions, i.e. by adding two hyperbolic terms to the undisturbed solution for the undamaged laminate. The difference between the initial guess and the final iteration in the case of local stresses can be large, but it is less than 1% for the case of shear modulus.

The cross-ply laminate here has transverse cracks with a uniform spacing ℓ_x in the 90° layer and longitudinal cracks with a uniform spacing ℓ_y in the 0° layer. The area between two transverse and two longitudinal cracks is called a "block". The origin of coordinates is set at the center of the block (Figs 6 and 7). In the case of pure shear loading with a shear force N_{xy} per unit length, the displacements in the x-direction are symmetric with respect to the x-axis and antisymmetric with respect to the y-axis; the displacements in the

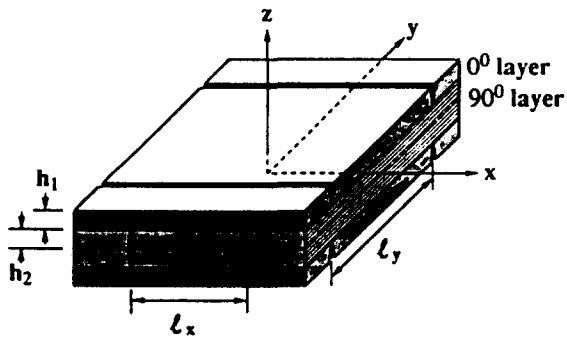

Fig. 6. Cross-ply [0_m/90_n], laminate with transverse and longitudinal cracks.

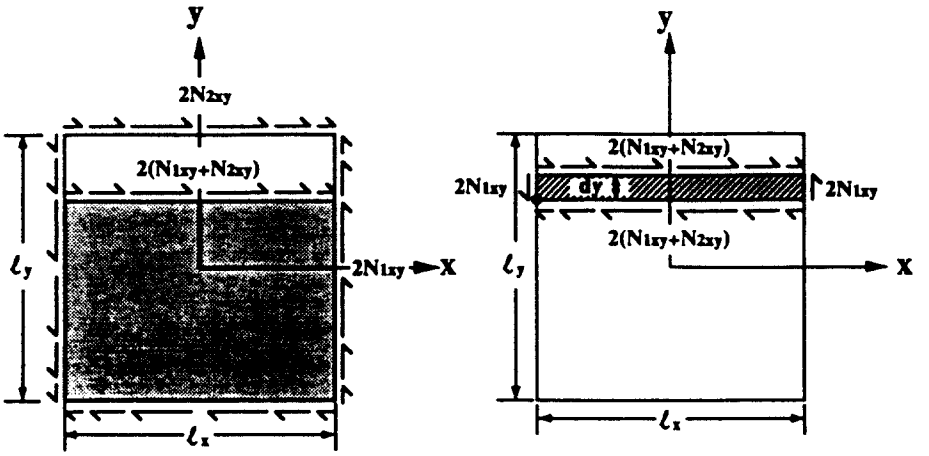

Fig. 7. Laminate element between two transverse and two longitudinal cracks and free body diagram.

y-direction are symmetric with respect to the y-axis and antisymmetric with respect to the x-axis. Thus,

$$\bar{v}_1 = \bar{v}_2 = 0, \quad \text{at } x = 0, \tag{40}$$

$$\bar{u}_1 = \bar{u}_2 = 0, \quad \text{at } y = 0, \tag{41}$$

$$\bar{u}_{1,x} = \bar{v}_{1,xx} = \bar{u}_{2,x} = \bar{v}_{2,xx} = 0, \quad \text{at } x = 0, \tag{42}$$

$$\bar{u}_{1,yy} = \bar{v}_{1,y} = \bar{u}_{2,yy} = \bar{v}_{2,y} = 0, \quad \text{at } y = 0. \tag{43}$$

The transverse cracks are at $x = \pm \ell_x/2$ and longitudinal cracks at $y = \pm \ell_y/2$. The stress-free boundary conditions are:

$$N_{2x} = N_{2xy} = 0, \quad \text{at } x = \pm \ell_x/2, \tag{44}$$

$$N_{1y} = N_{1xy} = 0, \quad \text{at } y = \pm \ell_y/2. \tag{45}$$

N_{1x} is anti-symmetric with respect to $x = \pm \ell_x/2$ and N_{2y} is anti-symmetric with respect to $y = \pm \ell_y/2$. These conditions give:

$$N_{1x} = 0, \quad \text{at } x = \pm \ell_x/2, \tag{46}$$

$$N_{2y} = 0, \quad \text{at } y = \pm \ell_y/2. \tag{47}$$

Around a block the external loading, N_{xy}, is defined as:

$$\frac{2}{\ell_x}\int_{-\ell_y/2}^{\ell_y/2} N_{2xy}(y = \pm \ell_y/2)\,dy = \frac{2}{\ell_y}\int_{-\ell_y/2}^{\ell_y/2} N_{1xy}(x = \pm \ell_x/2)\,dx = N_{xy}. \tag{48}$$

By making a cut through the block at y = constant, the total shear force along the section should equal the total shear loading at the bottom of the block because of the equilibrium condition of forces in the x-direction in the dotted area of Fig. 7:

$$2\int_{-\ell_y/2}^{\ell_y/2}(N_{1xy}+N_{2xy})\,dy = N_{xy}\ell_x = \text{constant}. \tag{49}$$

Now let us consider a slice from the block of width dy (Fig. 7). The total shear force at the top and bottom of the slice should be constant as was shown in eqn (49). Taking moments about an axis through the corner of the shaded area in Fig. 7 we obtain the conditions:

$$N_{1xy} = N_{xy}/2, \quad \text{at } x = \pm\ell_x/2. \tag{50}$$

Similarly,

$$N_{2xy} = N_{xy}/2, \quad \text{at } y = \pm\ell_y/2. \tag{51}$$

The force–displacement relations:

$$N_{1x} = Q_{11}\bar{u}_{1,x}+Q_{12}\bar{v}_{1,y}, \tag{52}$$

$$N_{1y} = Q_{12}\bar{u}_{1,x}+Q_{22}\bar{v}_{1,y}, \tag{53}$$

$$N_{1xy} = Q_{66}(\bar{u}_{1,y}+\bar{v}_{1,x}), \tag{54}$$

$$N_{2x} = Q_{22}\bar{u}_{2,x}+Q_{12}\bar{v}_{2,y}, \tag{55}$$

$$N_{2y} = Q_{12}\bar{u}_{2,x}+Q_{11}\bar{v}_{2,y}, \tag{56}$$

$$N_{2xy} = Q_{66}(\bar{u}_{2,y}+\bar{v}_{2,x}), \tag{57}$$

are introduced into eqns (44)-(47), (50) and (51) to obtain the following displacement gradients:

$$\bar{u}_{1,x} = -\frac{Q_{12}}{Q_{11}}\bar{v}_{1,y}, \quad \text{at } x = \pm\ell_x/2, \tag{58}$$

$$\bar{v}_{1,x} = -\bar{u}_{1,y}+\frac{N_{xy}}{2h_1Q_{66}}, \quad \text{at } x = \pm\ell_x/2, \tag{59}$$

$$\bar{u}_{2,x} = -\frac{Q_{12}}{Q_{22}}\bar{v}_{2,y}, \quad \text{at } x = \pm\ell_x/2, \tag{60}$$

$$\bar{v}_{2,x} = -\bar{u}_{2,y}, \quad \text{at } x = \pm\ell_x/2, \tag{61}$$

$$\bar{u}_{1,y} = -\bar{v}_{1,x}, \quad \text{at } y = \pm\ell_y/2, \tag{62}$$

$$\bar{v}_{1,y} = -\frac{Q_{12}}{Q_{22}}\bar{u}_{1,x}, \quad \text{at } y = \pm\ell_y/2, \tag{63}$$

$$\bar{u}_{2,y} = -\bar{v}_{2,x}+\frac{N_{xy}}{2h_2Q_{66}}, \quad \text{at } y = \pm\ell_y/2, \tag{64}$$

$$\bar{v}_{2,y} = -\frac{Q_{12}}{Q_{11}}\bar{u}_{2,x}, \quad \text{at } y = \pm\ell_y/2. \tag{65}$$

The finite difference iteration method was used to solve the governing equations for a quadrant of the block, for which we have sufficient boundary conditions (see Appendix).

The displacements obtained for the case of only one cracked layer (90°) are modified and used as the initial guess in the iteration process:

$$\bar{u}_1 = C_1 y, \tag{66}$$

$$\bar{v}_1 = C_2 x + \frac{h_2}{h_1} \frac{N_{xy}}{Q_{66} 2(h_1+h_2)\alpha \cosh(\alpha \ell_x/2)} \sinh(\alpha x), \tag{67}$$

$$\bar{u}_2 = C_1 y, \tag{68}$$

$$\bar{v}_2 = C_2 x - \frac{N_{xy}}{Q_{66} 2(h_1+h_2)\alpha \cosh(\alpha \ell_x/2)} \sinh(\alpha x), \tag{69}$$

where

$$C_1 + C_2 = \frac{N_{xy}}{Q_{66} 2(h_1+h_2)}, \quad \alpha = \sqrt{\frac{H_{22}}{Q_{66}} \left(\frac{1}{h_1} + \frac{1}{h_2}\right)} \quad \text{and} \quad H_{22} = \frac{3G_{13}G_{23}}{h_1 G_{13} + h_2 G_{23}}.$$

Adding similar hyperbolic disturbance terms for the longitudinal cracks to eqns (66) and (68) we obtain:

$$\bar{u}_1 = C_1 y - \frac{N_{xy}}{Q_{66} 2(h_1+h_2)\beta \cosh(\beta \ell_y/2)} \sinh(\beta y), \tag{70}$$

$$\bar{u}_2 = C_1 y + \frac{h_1}{h_2} \frac{N_{xy}}{Q_{66} 2(h_1+h_2)\beta \cosh(\beta \ell_y/2)} \sinh(\beta y), \tag{71}$$

where

$$\beta = \sqrt{\frac{H_{11}}{Q_{66}} \left(\frac{1}{h_1} + \frac{1}{h_2}\right)} \quad \text{and} \quad H_{11} = \frac{3G_{13}G_{23}}{h_2 G_{13} + h_1 G_{23}}.$$

The displacements given by eqns (67), (69), (70) and (71) are used as the initial guess in the finite difference iteration.

The iteration process is terminated when the maximum difference in displacement between the last iteration and the preceding one is less than 3% of the last value. The displacements obtained in this last iteration are introduced into eqns (52)–(57) to calculate the forces. The shear forces per unit length in each layer of a $[0_3/90_3]$, graphite/epoxy under pure shear loading are plotted along the x- and y-axes in Fig. 8. The difference between the initial guess and the last iteration is substantial near the crack.

The interlaminar stresses obtained by Tsai and Daniel (1991) are:

$$\begin{bmatrix} \tau_{ixz} \\ \tau_{iyz} \end{bmatrix} = \begin{bmatrix} N_{1x,x} + N_{1xy,y} \\ N_{1xy,x} + N_{1y,y} \end{bmatrix} = -\begin{bmatrix} N_{2x,x} + N_{2xy,y} \\ N_{2xy,x} + N_{2y,y} \end{bmatrix}, \tag{72}$$

$$\sigma_{iz} = \frac{h_1}{2}(\tau_{ixz,x} + \tau_{iyz,y}) = \frac{h_1}{2}(N_{1x,xx} + 2N_{1xy,xy} + N_{1y,yy}). \tag{73}$$

Along the sections $x = \pm \ell_x/2$, eqn (44) gives

$$N_{2xy} = N_{2x} = 0,$$

eqn (50) gives

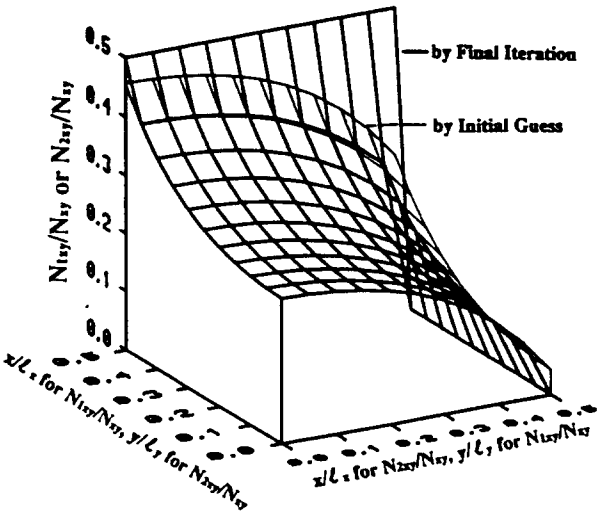

Fig. 8. Shear forces, N_{1xy} and N_{2xy}, by initial guess and final iteration of finite difference method.

$$N_{1xy} = N_{xy}/2,$$

and continuity and anti-symmetry with respect to $x = \pm \ell_x/2$ give

$$N_{1y} = 0.$$

Along the sections $y = \pm \ell_y/2$, eqn (45) gives

$$N_{1xy} = N_{1y} = 0,$$

eqn (51) gives

$$N_{2xy} = N_{xy}/2,$$

and continuity and anti-symmetry with respect to $y = \pm \ell_y/2$ give

$$N_{2x} = 0.$$

The above are introduced into eqns (72) and (73) to yield:

$$\begin{bmatrix} \tau_{xz} \\ \tau_{yz} \end{bmatrix} = \begin{bmatrix} N_{2x,x} + N_{2xy,y} \\ N_{1xy,x} + N_{1y,y} \end{bmatrix} = \begin{cases} \begin{bmatrix} \infty \\ \infty \end{bmatrix}, & \text{at } x = \pm \ell_x/2 \text{ and } y = \pm \ell_y/2 \\ \begin{bmatrix} 0 \\ 0 \end{bmatrix}, & \text{along } x = \pm \ell_x/2 \text{ or } y = \pm \ell_y/2 \end{cases}, \tag{74}$$

$$\sigma_{iz} = \infty, \quad \text{at } x = \pm \ell_x/2 \quad \text{and} \quad y = \pm \ell_y/2. \tag{75}$$

This result suggests that the cross-ply laminate with cross cracks cannot sustain any shear loading. In reality stresses do not become infinite or cross-ply specimens under shear would delaminate instantly at relatively low applied shear stresses.

Shear modulus reduction

The work done by the external shear loading is:

$$W = \int_{-\ell_x/2}^{\ell_x/2} N_{xy}|\bar{u}_2|(y = \ell_y/2)\,\mathrm{d}x + \int_{-\ell_x/2}^{\ell_x/2} N_{xy}|\bar{u}_2|(y = -\ell_y/2)\,\mathrm{d}x + \int_{-\ell_y/2}^{\ell_y/2} N_{xy}|\bar{v}_1|(x = \ell_x/2)\,\mathrm{d}y + \int_{-\ell_y/2}^{\ell_y/2} N_{xy}|\bar{v}_1|(x = -\ell_x/2)\,\mathrm{d}y. \quad (76)$$

If there is no damage in the laminate, the displacements will have no disturbance terms. This means that $\bar{u}_1 = \bar{u}_2 = C_1 y$ and $\bar{v}_1 = \bar{v}_2 = C_2 x$. In that case the work is given by:

$$W = \tfrac{1}{2} N_{xy}^2 \frac{\ell_x \ell_y}{Q_{66} 2(h_1 + h_2)}. \quad (77)$$

Using the initial guess to calculate the work we obtain:

$$W = \tfrac{1}{2} N_{xy}^2 \frac{\ell_x \ell_y}{\rho_G Q_{66} 2(h_1 + h_2)}, \quad (78)$$

where ρ_G is the laminate shear modulus reduction ratio given by the first guess as

$$\rho_G = \left[1 + \frac{h_2}{h_1}\frac{2}{\alpha \ell_x} \tanh\left(\frac{\alpha \ell_x}{2}\right) + \frac{h_1}{h_2}\frac{2}{\beta \ell_y} \tanh\left(\frac{\beta \ell_y}{2}\right)\right]^{-1}. \quad (79)$$

The shear forces along the boundary are introduced into eqn (76) and the work calculated is equated to that given by eqn (78) to obtain a value for the shear modulus reduction ratio ρ_G. When this was done it was found that the value of ρ_G obtained by the finite difference iteration was within 1% of the value given by eqn (79) which results from the initial guess. Thus, the first guess based on superposition of solutions for a single set of cracks is more than adequate for calculation of shear modulus reduction. The shear modulus reduction was calculated for a $[0_3/90_3]_s$ graphite/epoxy laminate and plotted versus transverse (90° layer) crack density for various values of longitudinal (0° layer) crack density in Fig. 9.

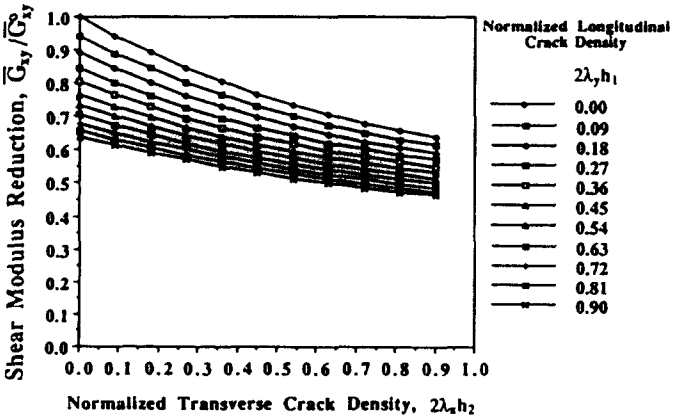

Fig. 9. Predicted shear modulus reduction as a function of normalized crack densities of $[0_3/90_3]_s$ cross-ply graphite/epoxy laminates.

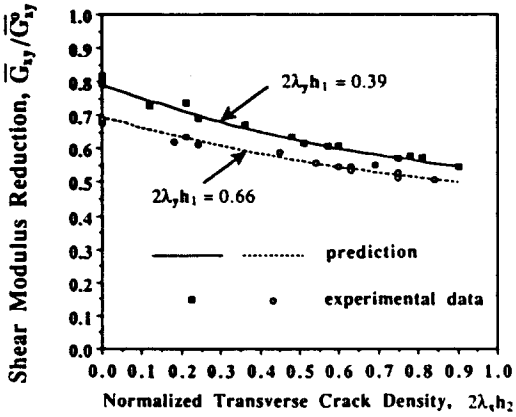

Fig. 10. Shear modulus reduction as a function of normalized crack densities of $[0_3, 90_3]_s$ cross-ply graphite epoxy laminates.

Experimental results

Graphite/epoxy cross-ply coupons of $[0_3/90_3]_s$ layup were tested to evaluate the predictions above. A plate of the $[0_3/90_3]_s$ laminate was first loaded normally to the 0° layer to introduce a set of cracks in that layer. Subsequently, coupons were machined from this precracked laminate with their axis parallel to the 0° layer. These coupons were subsequently loaded in steps to introduce progressively increasing cracking in the 90° layer. At each step, i.e. for each set of longitudinal and transverse cracks the shear modulus of the coupon was measured by the method described before. Results for shear modulus reduction are plotted in Fig. 10 versus transverse matrix cracking for two specific longitudinal crack densities. The experimental results are in excellent agreement with the analytical predictions.

SUMMARY AND CONCLUSIONS

An interlaminar-shear-stress analysis developed earlier for $[0_m/90_n]_s$ cross-ply laminates was applied to the case of a cracked cross-ply laminate under in-plane shear loading. For the case with only one layer (90°) cracked shear strains, forces and shear modulus reduction were obtained in closed form. Experimental results for shear modulus reduction due to cracking in the 90° layer only were in excellent agreement with predictions of this theory as well as those of Hashin (1985) and Tan and Nuismer (1989). The advantage of the proposed theory, as far as shear modulus is concerned, is that it does not need the exact state of stress in the laminate or any fracture criterion. The proposed approach is easier and more direct in its implementation.

For the case of laminates with both layers cracked the solution obtained by superposition in two directions of the closed-form solution for a single cracked layer was used as a first guess in a finite difference iteration process. The stress (force) distributions obtained by the final iteration were substantially different from those of the first guess. However, the shear modulus reduction calculated by the last iteration was within 1% of that obtained from the initial guess.

Acknowledgements—This work was sponsored by the Office of Naval Research (ONR). We are grateful to Dr Yapa Rajapakse of ONR for his encouragement and cooperation.

REFERENCES

Aboudi, J., Lee, S. W. and Herakovich, C. T. (1988). Three-dimensional analysis of laminates with cross cracks. *J. Appl. Mech.* **55**, 389–397.

Allen, D. H., Harris, C. E., Groves, S. E. and Norvell, R. G. (1988). Characterization of stiffness loss in crossply laminates with curved matrix cracks. *J. Comp. Mater.* **22**, 71–80.

Caslini, M., Zanotti, C. and O'Brien, T. K. (1987). Study of matrix cracking and delamination in glass/epoxy laminates. *J. Comp. Technol. Res.* **9**(4), 121–130.

Daniel, I. M. and Tsai, C.-L. (1991). Analytical experimental study of cracking in composite laminates under biaxial loading. *Comp. Engng* **1**(6), 355–362.
Dvorak, G. J., Laws, N. and Hejazi, M. (1985). Analysis of progressive matrix cracking in composite laminates, thermoelastic properties of a ply with cracks. *J. Comp. Mater.* **19**, 216–234.
Groves, S. E., Harris, C. E., Highsmith, A. L., Allen, D. H. and Norvell, R. G. (1987). An experimental and analytical treatment of matrix cracking in crossply laminates. *Expl Mech.* **27**, 73–79.
Hashin, Z. (1985). Analysis of cracked laminates: a variational approach. *Mech. Mater.* **4**, 121–136.
Hashin, Z. (1987). Analysis of orthogonally cracked laminates under tension. *J. Appl. Mech.* **54**, 872–879.
Herakovich, C. T., Aboudi, J., Lee, S. W. and Strauss, E. A. (1988). 2-D and 3-D damage effects in cross-ply laminates. *Mechanics of Composite Materials* (Edited by G. J. Dvorak and N. Laws), AMD-Vol. 92, pp. 143–147. New York.
Highsmith, A. L. and Reifsnider, K. L. (1982). Stiffness reduction mechanisms in composite laminates. In *Damage in Composite Materials, ASTM STP 775* (Edited by K. L. Reifsnider), pp. 103–117. American Society for Testing and Materials, PA.
Laws, N. and Dvorak, G. J. (1988). Progressive transverse cracking in composite laminates. *J. Comp. Mater.* **22**, 900–916.
Lee, J.-W. (1988). Damage development, property degradation and life prediction in composite laminates. Ph.D. Dissertation, Northwestern University.
Lee, J.-W. and Daniel, I. M. (1990). Progressive transverse cracking of crossply composite laminates. *J. Comp. Mater.* **24**(11), 1225–1243.
Lim, S. G. and Hong, C. S. (1989). Prediction of transverse cracking and stiffness reduction in cross-ply laminated composites. *J. Comp. Mater.* **23**, 695–713.
Ogin, S. L., Smith, P. A. and Beaumont, P. W. R. (1985). Matrix cracking and stiffness reduction during the fatigue of a [0/90], GFRP laminate. *Comp. Sci. Technol.* **22**, 23–31.
Sun, C. T. and Jen, K. C. (1987). On the effect of matrix cracks on laminate strength. *J. Reinforced Plast. and Comp.* **6**, 208–222.
Talreja, R. (1985). Transverse cracking and stiffness reduction in composite laminates. *J. Comp. Mater.* **19**, 355–375.
Tan, S. C. and Nuismer, R. J. (1989). A theory for progressive matrix cracking in composite laminates. *J. Comp. Mater.* **23**, 1029–1047.
Tsai, C.-L. and Daniel, I. M. (1991). The behavior of cracked crossply composite laminates under simple shear loading. *Comp. Engng* **1**, 3–11.
Tsai, C.-L., Daniel, I. M. and Lee, J.-W. (1990). Progressive matrix cracking of crossply composite laminates under biaxial loading. In *Microcracking-Induced Damage in Composites* (Edited by G. J. Dvorak and D. C. Lagoudas), Proc. of ASME 1990 Winter Annual Meeting, AMD-Vol. 111, MD-Vol. 22, pp. 9–18. ASME, New York.
Tsai, C.-L., Daniel, I. M. and Yaniv, G. (1990). Torsional response of rectangular composite laminates. *J. Appl. Mech.* **112**, 383–387.
Yaniv, G., Daniel, I. M. and Lee, J. W. (1989). Method for monitoring in-plane shear modulus in fatigue testing of composites. In *Test Methods for Design Allowable for Fibrous Composites, ASTM STP 1003* (Edited by C. C. Chamis), Vol. 2, pp. 276–284. American Society for Testing and Materials, PA.

APPENDIX: FINITE DIFFERENCE PROCEDURE FOR STRESS ANALYSIS OF LAMINATES WITH CRACKS IN BOTH LAYERS

The finite difference iteration method was used to solve the governing equations for a quadrant of the block, for which we have sufficient boundary conditions. This quadrant is cut into small elements of length Δx and height Δy, where $\Delta x = \ell_x/2M$ and $\Delta y = \ell_y/2N$ with M and N the number of elements in the x- and y-directions, respectively. The boundary conditions in the central difference formula used are (Fig. A1):

at $x = 0$,

$$\bar{u}_1(0, j) = \bar{u}_1(2, j), \tag{A1}$$

$$\bar{v}_1(0, j) = -\bar{v}_1(2, j), \tag{A2}$$

$$\bar{u}_2(0, j) = \bar{u}_2(2, j), \tag{A3}$$

$$\bar{v}_2(0, j) = -\bar{v}_2(2, j), \tag{A4}$$

at $y = 0$,

$$\bar{u}_1(i, 0) = -\bar{u}_1(i, 2), \tag{A5}$$

$$\bar{v}_1(i, 0) = \bar{v}_1(i, 2), \tag{A6}$$

$$\bar{u}_2(i, 0) = -\bar{u}_2(i, 2), \tag{A7}$$

$$\bar{v}_2(i, 0) = \bar{v}_2(i, 2), \tag{A8}$$

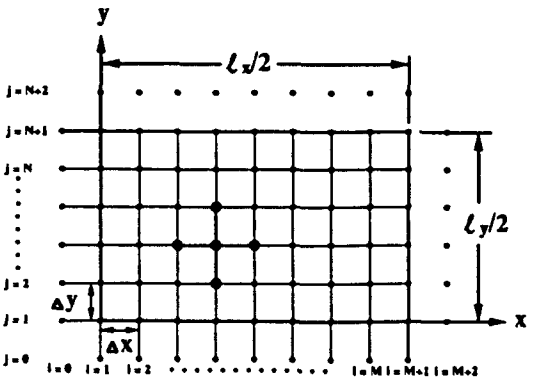

Fig. A1. Mesh of block for finite difference procedure.

at $x = \pm \ell_x/2$,

$$\bar{u}_1(M-2, j) = \bar{u}_1(M, j) - \frac{Q_{12}}{Q_{11}} \frac{\bar{v}_1(M+1, j+1) - \bar{v}_1(M+1, j-1)}{2\Delta y} 2\Delta x, \tag{A9}$$

$$\bar{v}_1(M+2, j) = \bar{v}_1(M, j) + \left[\frac{N_{xy}}{2h_1 Q_{66}} - \frac{\bar{u}_1(M+1, j+1) - \bar{u}_1(M+1, j-1)}{2\Delta y} \right] 2\Delta x, \tag{A10}$$

$$\bar{u}_2(M+2, j) = \bar{u}_2(M, j) - \frac{Q_{12}}{Q_{22}} \frac{\bar{v}_2(M+1, j+1) - \bar{v}_2(M+1, j-1)}{2\Delta y} 2\Delta x, \tag{A11}$$

$$\bar{v}_2(M+2, j) = \bar{v}_2(M, j) - \frac{\bar{u}_2(M+1, j+1) - \bar{u}_2(M+1, j-1)}{2\Delta y} 2\Delta x, \tag{A12}$$

and at $y = \pm \ell_y/2$,

$$\bar{u}_1(i, N+2) = \bar{u}_1(i, N) - \frac{\bar{v}_1(i+1, N) - \bar{v}_1(i-1, N)}{2\Delta x} 2\Delta y, \tag{A13}$$

$$\bar{v}_1(i, N+2) = \bar{v}_1(i, N) - \frac{Q_{12}}{Q_{22}} \frac{\bar{u}_1(i+1, N) - \bar{u}_1(i-1, N)}{2\Delta x} 2\Delta y, \tag{A14}$$

$$\bar{u}_2(i, N+2) = \bar{u}_2(i, N) + \left[\frac{N_{xy}}{2h_2 Q_{66}} - \frac{\bar{v}_2(i+1, N) - \bar{v}_2(i-1, N)}{2\Delta x} \right] 2\Delta y, \tag{A15}$$

$$\bar{v}_2(i, N+2) = \bar{v}_2(i, N) - \frac{Q_{12}}{Q_{11}} \frac{\bar{u}_2(i+1, N) - \bar{u}_2(i-1, N)}{2\Delta x} 2\Delta y. \tag{A16}$$

The governing equations (1)–(4) then become:

$$\left(2\frac{Q_{22}}{\Delta x^2} + 2\frac{Q_{66}}{\Delta y^2} + \frac{H_{11}}{h_2} \right) \bar{u}_2(i, j) - \frac{H_{11}}{h_2} \bar{u}_1(i, j) = Q_{22} \frac{\bar{u}_2(i+1, j) + \bar{u}_2(i-1, j)}{\Delta x^2} + Q_{66} \frac{\bar{u}_2(i, j+1) + \bar{u}_2(i, j-1)}{\Delta y^2}$$
$$+ (Q_{12} + Q_{66}) \frac{\bar{v}_2(i+1, j+1) - \bar{v}_2(i-1, j) - \bar{v}_2(i, j-1) + \bar{v}_2(i-1, j-1)}{4\Delta x \Delta y} \tag{A17}$$

$$\left(2\frac{Q_{11}}{\Delta x^2} + 2\frac{Q_{66}}{\Delta y^2} + \frac{H_{11}}{h_1} \right) \bar{u}_1(i, j) - \frac{H_{11}}{h_1} \bar{u}_2(i, j) = Q_{11} \frac{\bar{u}_1(i+1, j) + \bar{u}_1(i-1, j)}{\Delta x^2} + Q_{66} \frac{\bar{u}_1(i, j+1) + \bar{u}_1(i, j-1)}{\Delta y^2}$$
$$+ (Q_{12} + Q_{66}) \frac{\bar{v}_1(i+1, j+1) - \bar{v}_1(i-1, j) - \bar{v}_1(i, j-1) + \bar{v}_1(i-1, j-1)}{4\Delta x \Delta y} \tag{A18}$$

$$\left(2\frac{Q_{11}}{\Delta y^2} + 2\frac{Q_{66}}{\Delta x^2} + \frac{H_{22}}{h_2} \right) \bar{v}_2(i, j) - \frac{H_{22}}{h_2} \bar{v}_1(i, j) = Q_{11} \frac{\bar{v}_2(i, j+1) + \bar{v}_2(i, j-1)}{\Delta y^2} + Q_{66} \frac{\bar{v}_2(i+1, j) + \bar{v}_2(i-1, j)}{\Delta x^2}$$
$$+ (Q_{12} + Q_{66}) \frac{\bar{u}_2(i+1, j+1) - \bar{u}_2(i-1, j) - \bar{u}_2(i, j-1) + \bar{u}_2(i-1, j-1)}{4\Delta x \Delta y}, \tag{A19}$$

$$\left(2\frac{Q_{22}}{\Delta y^2}+2\frac{Q_{66}}{\Delta x^2}+\frac{H_{22}}{h_1}\right)\bar{v}_1(i,j)-\frac{H_{22}}{h_1}\bar{v}_2(i,j)=Q_{22}\frac{\bar{v}_1(i,j+1)+\bar{v}_1(i,j-1)}{\Delta y^2}+Q_{66}\frac{\bar{v}_1(i+1,j)+\bar{v}_1(i-1,j)}{\Delta x^2}$$
$$+(Q_{12}+Q_{66})\frac{\bar{u}_1(i+1,j+1)-\bar{u}_1(i-1,j)-\bar{u}_1(i,j-1)+\bar{u}_1(i-1,j-1)}{4\Delta x\,\Delta y}. \quad \text{(A20)}$$

From eqns (40) and (41) we obtain

$$\bar{v}_1(1,j)=\bar{v}_2(1,j)=0, \quad \text{at } x=0, \quad \text{(A21)}$$

$$\bar{u}_1(i,1)=\bar{u}_2(i,1)=0, \quad \text{at } y=0, \quad \text{(A22)}$$

and from eqns (58), (60), (63) and (65), we obtain:

$$\bar{u}_{1,xy}=-\frac{Q_{12}}{Q_{11}}\bar{v}_{1,yy}, \quad \text{at } x=\pm\ell_x/2, \quad \text{(A23)}$$

$$\bar{u}_{2,xy}=-\frac{Q_{12}}{Q_{22}}\bar{v}_{2,yy}, \quad \text{at } x=\pm\ell_x/2, \quad \text{(A24)}$$

$$\bar{v}_{1,xy}=-\frac{Q_{12}}{Q_{22}}\bar{u}_{1,xx}, \quad \text{at } y=\pm\ell_y/2, \quad \text{(A25)}$$

$$\bar{v}_{2,xy}=-\frac{Q_{12}}{Q_{11}}\bar{u}_{2,xx}, \quad \text{at } y=\pm\ell_y/2. \quad \text{(A26)}$$

Introducing eqns (A23) and (A24) into eqns (3) and (4), and eqns (A25), (A26) into eqns (1), (2) and applying the central difference formula we get:

$$\left[2\frac{Q_{11}-Q_{12}(Q_{12}+Q_{66})/Q_{22}}{\Delta x^2}+2\frac{Q_{66}}{\Delta x^2}+\frac{H_{22}}{h_2}\right]\bar{v}_2(i,j)-\frac{H_{22}}{h_2}\bar{v}_1(i,j)$$
$$=\left[Q_{11}-\frac{Q_{12}(Q_{12}+Q_{66})}{Q_{22}}\right]\frac{\bar{v}_2(i,j+1)+\bar{v}_2(i,j-1)}{\Delta y^2}+Q_{66}\frac{\bar{v}_2(i+1,j)+\bar{v}_2(i-1,j)}{\Delta x^2}, \quad \text{at } x=\pm\ell_x/2, \quad \text{(A27)}$$

$$\left[2\frac{Q_{22}-Q_{12}(Q_{12}+Q_{66})/Q_{11}}{\Delta y^2}+2\frac{Q_{66}}{\Delta x^2}+\frac{H_{22}}{h_1}\right]\bar{v}_1(i,j)-\frac{H_{22}}{h_1}\bar{v}_2(i,j)$$
$$=\left[Q_{22}-\frac{Q_{12}(Q_{12}+Q_{66})}{Q_{11}}\right]\frac{\bar{v}_1(i,j+1)+\bar{v}_1(i,j-1)}{\Delta y^2}+Q_{66}\frac{\bar{v}_1(i+1,j)+\bar{v}_1(i-1,j)}{\Delta x^2}, \quad \text{at } x=\pm\ell_x/2, \quad \text{(A28)}$$

$$\left[2\frac{Q_{22}-Q_{12}(Q_{12}+Q_{66})/Q_{11}}{\Delta x^2}+2\frac{Q_{66}}{\Delta y^2}+\frac{H_{11}}{h_2}\right]\bar{u}_2(i,j)-\frac{H_{11}}{h_2}\bar{u}_1(i,j)$$
$$=\left[2\frac{Q_{22}}{\Delta x^2}+2\frac{Q_{66}}{\Delta y^2}+\frac{H_{11}}{h_2}\right]\frac{\bar{u}_2(i+1,j)+\bar{u}_2(i-1,j)}{\Delta x^2}+Q_{66}\frac{\bar{u}_2(i,j+1)+\bar{u}_2(i,j-1)}{\Delta y^2}, \quad y=\pm\ell_y/2, \quad \text{(A29)}$$

$$\left[2\frac{Q_{11}-Q_{12}(Q_{12}+Q_{66})/Q_{22}}{\Delta x^2}+2\frac{Q_{66}}{\Delta y^2}+\frac{H_{11}}{h_1}\right]\bar{u}_1(i,j)-\frac{H_{11}}{h_1}\bar{u}_2(i,j)$$
$$=\left[Q_{11}-\frac{Q_{12}(Q_{12}+Q_{66})}{Q_{22}}\right]\frac{\bar{u}_1(i+1,j)+\bar{u}_1(i-1,j)}{\Delta x^2}+Q_{66}\frac{\bar{u}_1(i,j+1)+\bar{u}_1(i,j-1)}{\Delta y^2}, \quad y=\pm\ell_y/2. \quad \text{(A30)}$$

Equations (A19) and (A20) are used to calculate $\bar{v}_1(i,j)$ and $\bar{v}_2(i,j)$ when $i\neq 1$ or $M+1$. When $i=M+1$, we use eqns (A27) and (A28). When $i=1$, $\bar{v}_1(i,j)=\bar{v}_2(i,j)=0$. Equations (A17) and (A18) are used to calculate $\bar{u}_1(i,j)$ and $\bar{u}_2(i,j)$ when $j\neq 1$ or $N+1$. When $j=N+1$, we use equations (A29) and (A30). When $j=1$, $\bar{u}_1(i,j)=\bar{u}_2(i,j)=0$. The values on the right-hand side of eqns (A17)–(A20) and eqns (A27)–(A30) are given by the initial guess for the first iteration or by the previous iteration for subsequent iterations. There is a problem at the singular points $x=\pm\ell_x/2$ and $y=\pm\ell_y/2$. Equations (A10) and (A13) do not hold simultaneously. The same condition is true for eqns (A12) and (A15). This type of problem is inherent in the finite difference method. Equations (A10) and (A15) are selected for the corner. Different combinations were tried. It was shown that as long as ΔX and Δy are small in comparison with ℓ_x and ℓ_y the solutions are very close to each other.

By using the backward difference method we can write the interlaminar stresses of eqns (72) and (73) as:

$$\begin{bmatrix} \tau_{xz}(i,j) \\ \tau_{yz}(i,j) \end{bmatrix} = \begin{bmatrix} \dfrac{N_{1x}(i,j)-N_{1x}(i-1,j)}{\Delta x} + \dfrac{N_{1xy}(i,j)-N_{1xy}(i,j-1)}{\Delta y} \\ \dfrac{N_{1xy}(i,j)-N_{1xy}(i-1,j)}{\Delta x} + \dfrac{N_{1y}(i,j)-N_{1y}(i,j-1)}{\Delta y} \end{bmatrix}, \tag{A31}$$

$$\sigma_{iz}(i,j) = \frac{h_1}{2}\left[\frac{N_{1x}(i,j)-2N_{1x}(i-1,j)-N_{1x}(i-2,j)}{\Delta x^2}\right.$$

$$\left. +2\,\frac{N_{1xy}(i,j)-N_{1xy}(i-1,j)-N_{1xy}(i,j-1)+N_{1xy}(i-1,j-1)}{\Delta x\,\Delta y} + \frac{N_{1y}(i,j)-2N_{1y}(i,j-1)-N_{1y}(i,j-2)}{\Delta y^2}\right]. \tag{A32}$$